

# Reynolds Number Effects on the Turbulence Field in Compressible Boundary Layers

M. Acharya,\* C.C. Horstman,† and M.I. Kussoy‡  
NASA Ames Research Center, Moffett Field, Calif.

Detailed experiments were conducted in a zero pressure gradient, supersonic turbulent boundary layer, including measurements of the three components of velocity fluctuations and the turbulent shear stress, for Reynolds numbers ranging from  $11.7$  to  $105 \times 10^6$  at a freestream Mach number of  $2.3$ . The mean flow measurements established the fully developed and equilibrium nature of the boundary layer. Measurements of the turbulence field show that the vertical and transverse fluctuations  $\langle v' \rangle$  and  $\langle w' \rangle$  are essentially equal throughout the boundary layer at all Reynolds numbers, a feature that is different from observations in incompressible flows. The data show that the boundary layer exhibits similarity in the turbulence profiles for the entire Reynolds number range and agrees with previous compressible and incompressible data using Morkovin's scaling to account for compressibility effects.

## Nomenclature

$e$	= sensor voltage
$f$	= frequency
$k$	= turbulent energy, $(\overline{u'^2} + \overline{v'^2} + \overline{w'^2})/2$
$M$	= Mach number
$p$	= pressure
$Re$	= Reynolds number
$S_{T_0}$	= sensor sensitivity to total temperature
$S_{\rho u}$	= sensor sensitivity to mass flux
$u$	= streamwise velocity component
$u_\tau$	= skin-friction velocity at wall
$v$	= vertical velocity component
$w$	= transverse velocity component
$y$	= vertical coordinate (normal to wall)
$y^+$	= transformed nondimensional vertical coordinate
$\delta$	= boundary-layer thickness
$\delta^*$	= boundary-layer displacement thickness
$\theta$	= boundary-layer momentum thickness
$\rho$	= density
$\tau$	= shear stress

## Subscripts

$e$	= boundary-layer edge
$T$	= total
$x$	= based on distance from nozzle throat
$w$	= wall
$\delta$	= based on boundary-layer thickness
$\theta$	= based on boundary-layer momentum thickness

## Superscripts

$( )'$	= fluctuating value
$\langle \rangle$	= root mean square
$( )$	= time averaged value

## Introduction

IN a recent survey<sup>1</sup> of compressible turbulence measurements, Sandborn has examined studies of zero pressure gradient supersonic turbulent boundary layers that have been

reported in the literature. These experiments, and a few others which have been reported since Sandborn's review, have presented data on the turbulence field; however, most of them have been limited to a part of the fluctuating field, and all of them together cover only a limited range of Reynolds numbers.

Detailed information on the turbulence field in compressible turbulent boundary layers is of value in light of current trends in the computation of compressible flowfields, which are directed toward the development and refinement of sophisticated numerical codes. These codes are ultimately expected to provide the capability to predict flows about realistic aerospace configurations, with the possible presence of shocks and flow separation. Such codes utilize the Navier-Stokes equations, together with a turbulence model to provide closure. The development of a suitable model is proving to be the pacing item in this effort.

Concurrent with the development of turbulence models, it is essential to conduct experiments that would provide guidelines for such development, and also help in the evaluation of different computational techniques. Such an approach has been adopted at Ames Research Center as described by Marvin.<sup>2</sup>

At present there is a considerable effort to develop Reynolds stress-equation or higher-order turbulence closure models. In spite of their increased complexity, stress-equation models have inherent advantages over the simpler two-equation and eddy-viscosity models, because they are expected to provide a more realistic modeling of complex flows,<sup>3,4</sup> in which features such as three dimensionality, separation, and flow curvature could be present. Stress-equation models would provide a detailed prediction of the turbulence field, including the individual components of the Reynolds stress tensor. In light of this, it would be useful to conduct experiments detailing the behavior of the turbulence field for a wide range of flow conditions such as Reynolds and Mach number.

This paper presents the results of detailed measurements of the turbulence field in a supersonic zero pressure gradient, turbulent boundary layer over a Reynolds number range of  $11.7$  to  $105 \times 10^6$ . The data were obtained in sufficient detail to assess the Reynolds number effects, document the flowfield, and serve as a basis for the comparison of computations using different higher-order turbulence models. The study was also extended at a single Reynolds number to include measurements in a range of adverse pressure gradients approaching separation. These results have been reported by Acharya et al.<sup>5</sup>

Received May 5, 1978; revision received Nov. 28, 1978. This paper is declared a work of the U.S. Government and therefore is in the public domain.

Index categories: Boundary Layers and Convective Heat Transfer-Turbulent; Supersonic and Hypersonic Flow.

\*NRC Research Associate. Now, Scientist, Aerodynamics Division, National Aeronautical Laboratory, Bangalore, India.

†Assistant Chief, Experimental Fluid Dynamics Branch. Associate Fellow AIAA.

‡Research Scientist. Member AIAA.

## Description of Experiment

### Flow Facility

The experiments were conducted in the NASA Ames High Reynolds Number Channel. This is an air-charged, blowdown facility consisting of a large settling tank with flow conditioning screens and interchangeable test sections and nozzles, each designed to produce a particular flow. For the present study, a supersonic nozzle and a constant diameter (24.77-cm) test section 270-cm long were used. The nominal freestream test conditions were total temperature, 270K; total pressure, 0.33 to 3 atm; freestream unit Reynolds number, 4 to  $35 \times 10^6 \text{ m}^{-1}$ ; and freestream Mach number, 2.3. The wall temperature was 278K. For each test condition a slight Mach number gradient ( $-0.05/\text{m}$ ) existed in the test section because of boundary-layer growth on the wall. The useful test time varied from 5 to 60 min, depending on the total pressure.

Instrumentation ports, into which interchangeable plugs could be inserted were located at 25.4-cm intervals along the test section. The plugs 3.81 cm in diameter, were machined in place to fit flush (a maximum step of  $3 \mu\text{m}$ ) with the inner cylindrical surface. One plug was fitted with a survey mechanism built to accommodate various hot-wire and pressure probes. The others contained static pressure taps and flush-mounted thermocouples. Additional static pressure taps were located 90 deg around the test section at selected stations to verify flow symmetry. The boundary-layer profile data presented in this paper were obtained 290-cm downstream from the nozzle throat. The average surface roughness on the inside of the test section was approximately  $0.4 \mu\text{m}$ , an order of magnitude less than the minimum viscous sublayer thickness encountered during the present tests.

### Mean and Surface Measurements

The details of the construction, calibration, and use of the pressure and total temperature probes for the measurement of skin friction, mean velocities, static pressure and total temperature profiles have been presented in Ref. 6. The experimental uncertainties in surface-pressure and skin-friction measurement were estimated to be  $\pm 5\%$  and  $\pm 15\%$ , respectively. The measured values of total temperature across the boundary layer were essentially constant (the maximum variation was 0.5%). The experimental uncertainties in the mean flowfield data were  $\pm 0.5\%$  for the total temperature,  $\pm 10\%$  for the static pressure,  $\pm 6\%$  for the static temperature,  $\pm 12\%$  for density, and  $\pm 3\%$  for the velocity. The uncertainty in  $y$ , the distance from the wall, was  $\pm 0.01 \text{ cm}$ .

### Fluctuating Measurements

Single hot-wire and dual-wedge hot-film probes were used to obtain the three fluctuating velocity components and turbulent shear stresses.<sup>6</sup> A single hot wire ( $10 \mu\text{m}$ -diam and 0.15-cm long) was used for calibration purposes. A second single hot wire of the same dimensions, but supported with an epoxy film (to prevent wire breakage and signal distortion due to vibration and strain gaging effects) was used to measure mass flow and total temperature fluctuations. For the present test series a single epoxy-backed wire survived over 35 boundary-layer traverses. A commercially available dual-wedge film probe (0.11-cm in diameter) was used to obtain the correlation coefficients and the instantaneous ratios of the vertical and transverse velocities to the mass flow fluctuations. These probes were operated with constant-temperature anemometers. Spectrum analysis established that the useful frequency range for all probes used was over 100 KHz and subsequent data analysis indicated that less than 1% of the flow energy was contained in frequencies above 80 KHz.

The principal difficulty in using hot wires and films in compressible flow is that the sensor responds to velocity, density, and total temperature fluctuations, and, in general, exhibits a different sensitivity to each one. However, it has

been shown by Morkovin<sup>7</sup> for supersonic speeds and by Horstman and Rose<sup>8</sup> for transonic speeds that the density and velocity sensitivities are equal for specific test conditions. It has been shown in Ref. 8 that, provided the Reynolds number based on sensor diameter is greater than 20 and the temperature overhear is greater than 0.4, the sensors respond to mass flow rather than density and velocity separately, at all Mach numbers. For the present investigation, the minimum sensor Reynolds number was 30, and the temperature overhears were usually greater than 1.0, both well within the required ranges. Both the bare wire and epoxy-backed probes were calibrated and used to measure the mass flow fluctuations. (The calibrations were performed both in the freestream, varying the tunnel total pressure, and by traverses through the previously measured boundary layer.) Since the epoxy-backed wire could be affected by thermal feedback problems which cause changes in the sensor sensitivity, corrections to the epoxy-backed probe sensitivity coefficients were determined by comparison of the measurements obtained by the two probes. These corrections were found to be a function of a probe Reynolds number, varying from 30% at the lowest to 5% at the highest Reynolds numbers tested. Details of the calibration techniques are described in Ref. 9.

The dual-wedge film probes were used to measure the vertical and transverse velocity fluctuations and the turbulent shear stresses. By operating the probe at a single high overhear and measuring only ratios of fluctuating voltages (and their sums and differences) the only calibration measurements required are relative measurements of the mean voltages to insure that the two films had equal sensitivities. The data reduction techniques and equations used to obtain the Reynolds shear stress from the measured quantities are described in Ref. 8. A Prandtl number of 0.9 was assumed in the data reduction procedure.

Horizontal velocity fluctuations were obtained from the mass flux fluctuations assuming negligible total temperature and pressure fluctuations. The latter assumption has been verified by Johnson and Rose<sup>10</sup> at the present Mach number. A 1% fluctuation in total temperature would result in a maximum error of 10% in the inferred velocity fluctuation. For the present investigation the total temperature fluctuations were much less than 1% (see below).

The epoxy-backed normal wire was used to measure the mass flow and total temperature fluctuations at three points within the boundary layer, using the mode diagram approach developed by Kovaszny.<sup>11,12</sup> The results are shown in Fig. 1. The temperature sensitivity  $S_{T_0}$  decreases with increasing overhear while the mass flux sensitivity  $S_{\rho u}$  remains relative constant. Thus, the intercept on the ordinate, where  $(S_{\rho u}/S_{T_0}) \rightarrow 0$ , gives the intensity of the total temperature fluctuations while the slope of the curve at high values of  $S_{\rho u}/S_{T_0}$  yields the intensity of the mass flux fluctuations. Least-square curve fits to the data (the solid lines in Fig. 1) indicate negligible total temperature fluctuations across the entire boundary layer. However, it should be noted that at very low overhears, a constant-temperature system has poor frequency response and the density and velocity sensitivities may no longer be equal, so that errors could be introduced in a measurement of the total temperature fluctuations. Least-square curve fits were also obtained for these data, neglecting the data obtained at the lower overhears. Although the accuracy of extrapolating high overhear data to low overhears may be questioned, the results indicated that the level of total temperature fluctuations was of the order of 1% for  $y/\delta = 0.04$  and 0.20 and again negligible for  $y/\delta = 0.70$ . The mass-flux total-temperature correlation coefficients were approximately equal to 0.5, and at the higher overhears the sensor responded predominantly to the mass flux fluctuations. With the exception of the data for the modal analysis plots discussed earlier, all probes were operated at high overhears ( $S_{\rho u}/S_{T_0} > 1.5$ ), where the total temperature fluctuations could be neglected.

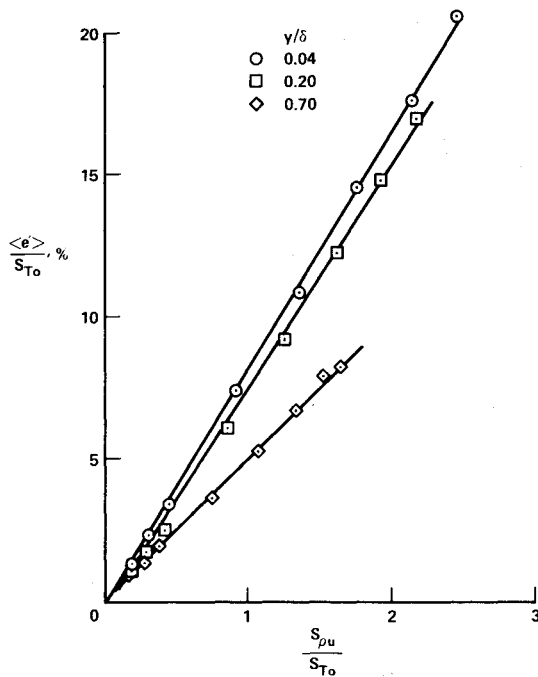


Fig. 1 Modal analysis comparing three positions in the boundary layer;  $Re_x = 35.3 \times 10^6$ .

The experimental uncertainties in the fluctuating flowfield quantities due to the various assumptions employed and calibration errors were  $\pm 15\%$  for the fluctuating velocity components and  $\pm 20\%$  for the turbulent stresses. Error bands representing these experimental uncertainties are shown on the figures containing the fluctuating data. A tabulation of all mean and fluctuating data contained in this paper is presented in Ref. 6.

### Results and Discussion

The measured boundary-layer parameters for the nominal test conditions described earlier are summarized in Table 1. Measurements were made for three values of total pressure  $P_T$ , resulting in freestream Reynolds numbers, based on the distance from the sonic throat, of  $11.7$ ,  $35.3$ , and  $105 \times 10^6$ . The corresponding momentum thickness Reynolds number also varied by about one order of magnitude, the maximum value being  $8.28 \times 10^4$ . The boundary-layer thickness  $\delta$  was defined as the thickness determined by extrapolation of the measured velocity profiles in the power-law form  $\ln u/u_e$  vs  $\ln y$  to  $u/u_e = 1.0$  (see Ref. 13).

Figure 2 shows the mean velocity data for the three Reynolds numbers, plotted in the conventional wall coordinates. The data were transformed into incompressible coordinates using the Van Driest II transformation. Neglecting the first few points near the wall for each Reynolds number (because of possible probe interference effects), the good agreement with the law of the wall verifies the presence of a fully developed flow for the inner half of the boundary layer. To verify fully developed flow for the other half of the boundary layer the same data, scaled by the outer variables, are shown in Fig. 3. The similarity in profiles is quite good except for a small portion of the highest Reynolds number

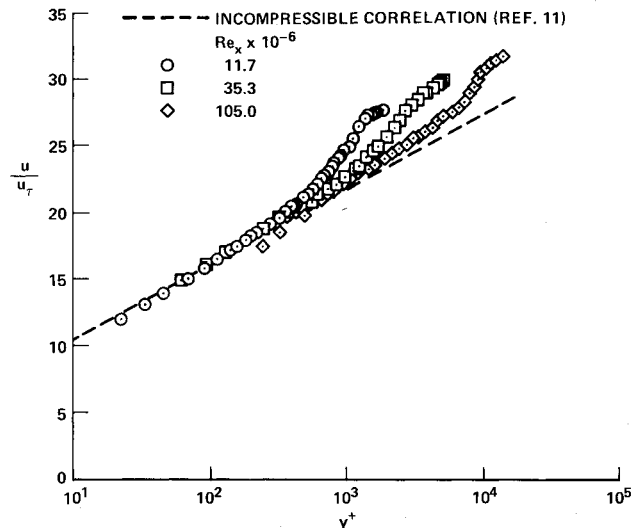


Fig. 2 Law-of-the-wall correlations in compressible coordinates using the Van Driest transformation.

flow near  $y/\delta = 0.6$ . This variation could possibly be attributable to small nonequilibrium effects originating in the wind tunnel nozzle. Since turbulence memory distances can be significantly longer than corresponding mean flow memory distances<sup>4</sup> these nonequilibrium effects could be more pronounced in the turbulence field. With this small exception, the mean velocity measurements serve to establish the presence of a fully developed equilibrium turbulent boundary layer.

Typical power spectra distributions nondimensionalized by the power contained in the interval 0 to 400 Hz, obtained for the commercial dual-wedge probes are shown in Fig. 4. Comparison of the vertical and transverse velocity spectra with the mass flux spectrum (Fig. 4a) shows that there is proportionally more energy associated with the smaller scales for the two velocity components. Since the horizontal velocity cannot be measured directly in a compressible flow with a hot wire, its spectra cannot be compared with the other components. Changes in Reynolds number had only a small effect on the measured spectra (Fig. 4b).

The three components of rms turbulent velocity fluctuations at a freestream Reynolds number of  $11.7 \times 10^6$  are shown in Fig. 5. An examination of the profiles shows that the vertical velocity fluctuations  $\langle v' \rangle$  and the transverse fluctuations  $\langle w' \rangle$  are essentially equal except near the wall. This is in disagreement with previous incompressible measurements such as those by Klebanoff<sup>14</sup> where  $\langle w' \rangle$  was found to be at least 20% greater than  $\langle v' \rangle$  across the entire boundary layer. However, the only other measurements of  $\langle w' \rangle$  in compressible flow (Acharya<sup>15</sup> at  $M_e = 0.45$ , Horstman and Rose<sup>7</sup> at  $M_e = 0.78$ , and Mikulla and Horstman<sup>16</sup> at  $M = 7.0$ ) show a similar tendency in that  $\langle w' \rangle$  was only a few percent greater than  $\langle v' \rangle$  in the outer half of the boundary layer for the  $M_e = 0.45$  and  $0.78$  data, and equal to  $\langle v' \rangle$  across the entire boundary layer for the  $M_e = 7.0$  data. The fluctuation data at freestream Reynolds numbers of  $35.3 \times 10^6$  and  $105 \times 10^6$  also reveal very similar trends.

Another possible reason for this disagreement with Klebanoff's results is the effect of transverse curvature. For

Table 1 Measured boundary-layer parameters

$P_T$ atm	$M_e$	$u_e$ , m/s	$\delta$ , cm	$\delta^*$ , cm	$\theta$ , cm	$\tau_w$ , g/cm <sup>2</sup>	$u_\tau$ , m/s	$Re_{\tau}$ , $\times 10^{-6}$	$Re_\theta$ , $\times 10^{-4}$
0.33	2.21	525.72	4.7	0.970	0.264	0.165	19.81	11.7	1.04
1.0	2.26	530.41	4.7	0.846	0.233	0.430	19.84	35.3	2.82
3.0	2.34	539.77	4.7	0.854	0.228	1.09	19.20	105	8.28

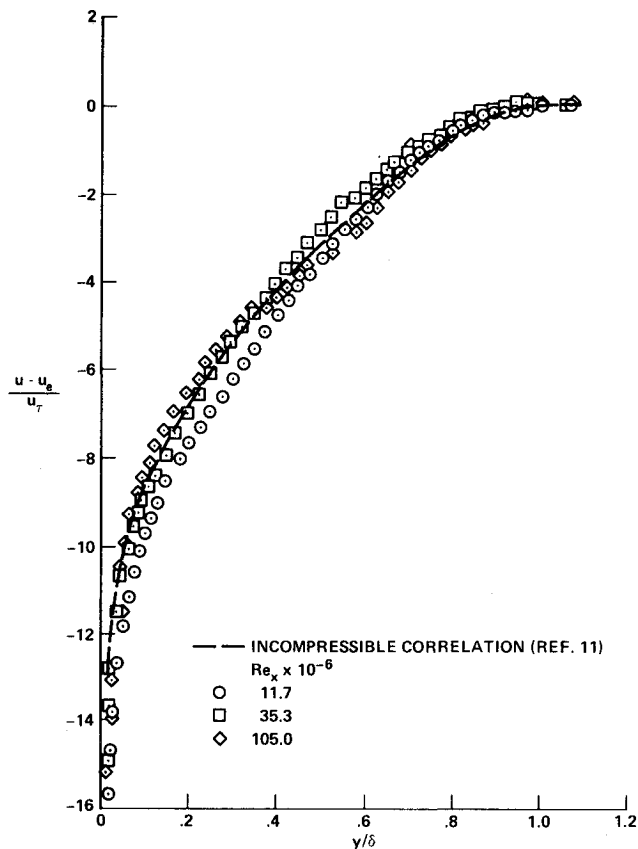
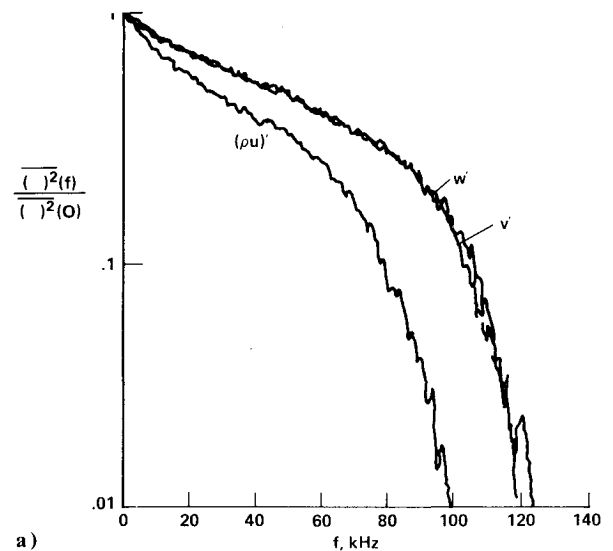


Fig. 3 Velocity-defect profiles in incompressible coordinates using the Van Driest transformation.

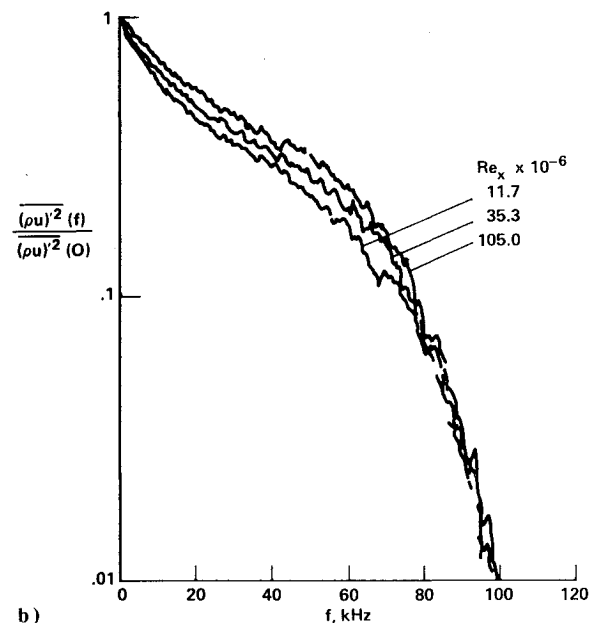
both the present data and the results of Ref. 16 the ratio of the boundary-layer thickness to the wall transverse radius of curvature is  $\sim 0.35$ . Klebanoff's results were obtained on a flat plate. Although the mean flow profiles for the present case and Ref. 16 agree with flat-plate data, the effects of transverse curvature on the turbulent fluctuations, especially  $\langle v' \rangle$  and  $\langle w' \rangle$ , may be important. Additional measurements of  $\langle v' \rangle$  and  $\langle w' \rangle$  in a supersonic flat-plate boundary layer would be required to resolve this issue.

Figures 6-8 compare the fluctuations at the different Reynolds numbers. Figure 6 shows the data for the streamwise fluctuations  $\langle u' \rangle$ . While the Reynolds number has been changed by almost one order of magnitude, the profiles remain essentially unchanged. From Figs. 7 and 8, it is seen that  $\langle v' \rangle$  and  $\langle w' \rangle$  also exhibit the same behavior with change in Reynolds number. Figure 9 shows the variation of the turbulent kinetic energy per unit mass across the boundary layer at the three Reynolds numbers, confirming that the turbulence intensity profiles attain similarity at high Reynolds numbers. (For the highest Reynolds number, measurements of  $\langle v' \rangle$  and shear stress were not obtained in the outer half of the boundary layer because of the power limitations of the anemometry system at high overheats for the dual-wedge probe.)

Morkovin<sup>17</sup> originally proposed that the effects of compressibility on the turbulent fluctuations were passive, and could be accounted for by scaling the data using the wall shear stress and local mean density. This has been shown to be valid for the horizontal velocity fluctuations in subsonic and supersonic compressible flows by Acharya,<sup>15</sup> Sandborn,<sup>1</sup> and Johnson and Rose.<sup>10</sup> To test the present data with this scaling, the  $\langle u' \rangle$  fluctuations normalized in this manner are compared with previous incompressible and compressible data in Fig. 10. The Mach and Reynolds numbers of each set of data are indicated in the figure key. The present data are in general agreement (within the experimental accuracy of



a)



b)

Fig. 4 Nondimensionalized power spectra distributions;  $y/\delta = 0.21$ : a) comparison of fluctuating mass flux and vertical and transverse velocity components— $Re_x = 105 \times 10^6$ ; b) comparison of the mass flux fluctuations at three Reynolds numbers.

$\pm 15\%$ ) with the previous data. Over the central portion of the boundary layer ( $y/\delta \approx 0.6$ ) the present highest Reynolds number data are slightly high, which could be due to the nonequilibrium effects discussed earlier. The total spread in the present data at  $y/\delta = 0.5$  due to Reynolds number is 25% compared to 10% when these data are not scaled in this manner (Fig. 6). Whether this increase is due to the scaling or to inaccuracies in the data cannot be determined at this time.

The same scaling has been applied to the present vertical velocity fluctuations together with previous data and is shown in Fig. 11. No apparent correlation is observed. The measurement of  $\langle v' \rangle$  with hot wires poses problems of probe resolution and is also subject to fairly large error resulting from velocity gradients across the sensor.<sup>18</sup> These could be the main reasons for the large differences seen in the data, especially in the inner regions. Even the incompressible data are inconsistent among themselves. Johnson and Rose<sup>10</sup> also made an independent measurement of the  $\langle v' \rangle$  profile using a laser velocimeter. These data were in disagreement with their

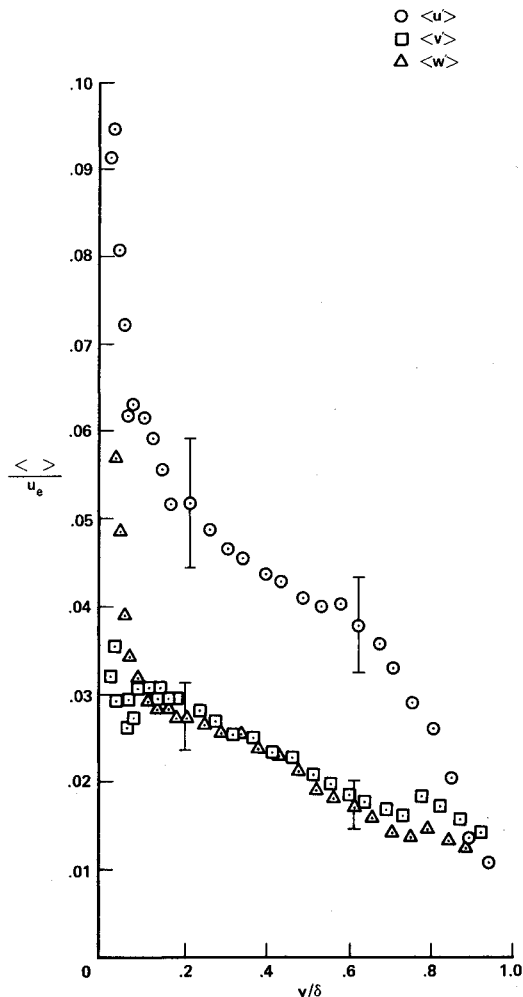


Fig. 5 Distributions of the rms streamwise, vertical, and transverse velocity fluctuations across the boundary layer,  $Re_x = 11.7 \times 10^6$ .

hot-wire measurements but were in good agreement with Zoric's<sup>19</sup> data. It is difficult to draw definite conclusions regarding the scaling of  $\langle v' \rangle$  based on the available data.

As a check on the present data, the measured shear stress distribution at a freestream Reynolds number of  $35.3 \times 10^6$  is compared in Fig. 12 with the expected shear stress distribution obtained from integration of the mean-flow data. The observed differences are well within experimental accuracy except near the wall ( $y/\delta < 0.25$ ) where probe interference effects may be present. These probe interference effects only apply to the turbulent shear stress measurements and occur when the local Mach number approaches unity (see Ref. 6).

The turbulent shear stress data at all three Reynolds numbers are shown normalized by the wall shear stress in Fig. 13, together with the data of Klebanoff, Acharya, and Johnson and Rose. As was found with the  $\langle v' \rangle$  data, the scatter in the shear stress data are too large to verify this scaling. Sandborn<sup>1</sup> constructed a "best estimate" shear stress distribution by solving the momentum equation for the shear stress, which he then evaluated using mean-flow profiles, with the assumption that these profiles were self-similar in the streamwise direction. This "best estimate" was independent of Mach and Reynolds number. This estimate fits the present shear stress data within their experimental accuracy except near the wall ( $y/\delta < 0.25$ ) where probe interference effects may be present. Measurements revealed that the  $-\rho u' w'$  component of the turbulent stress tensor was essentially zero throughout the boundary layer, at all three Reynolds numbers, as expected.

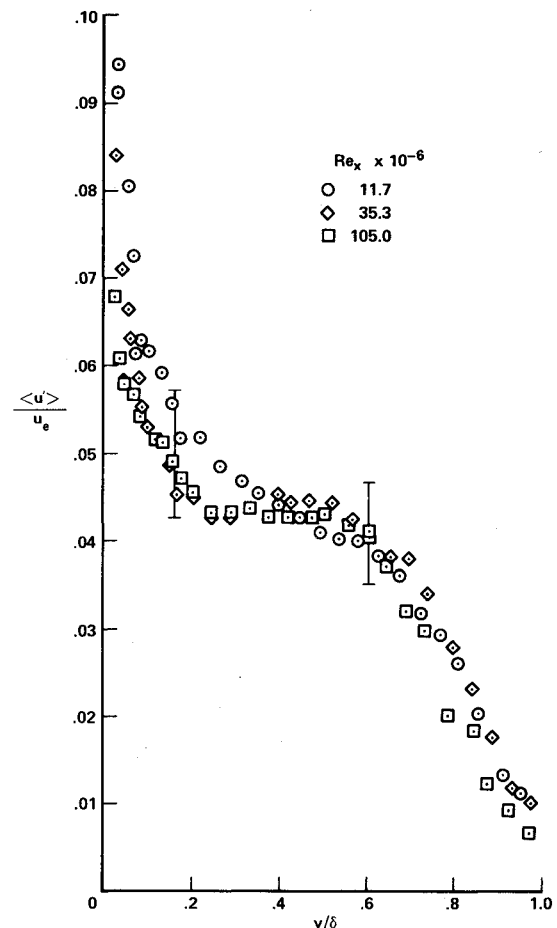


Fig. 6 Distributions of the rms streamwise velocity fluctuations for various Reynolds numbers.

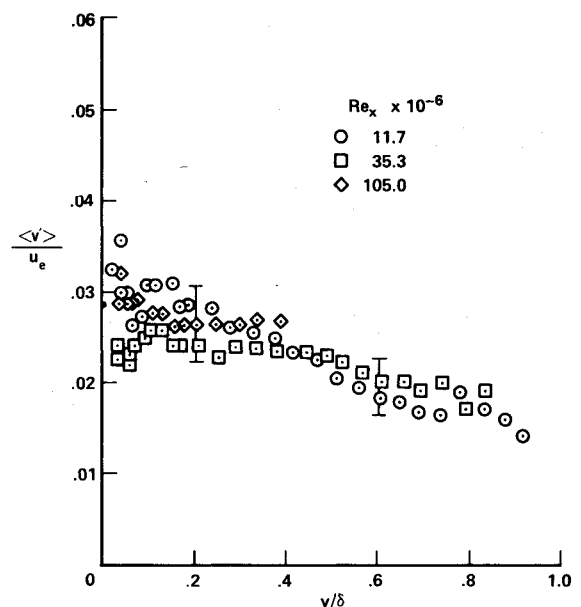


Fig. 7 Distributions of the rms vertical velocity fluctuations for various Reynolds numbers.

## Conclusions

A zero pressure gradient supersonic turbulent boundary layer has been investigated in detail for a wide range of Reynolds numbers. The measurements included mean-flow profiles and profiles of the three turbulent velocity fluctuation

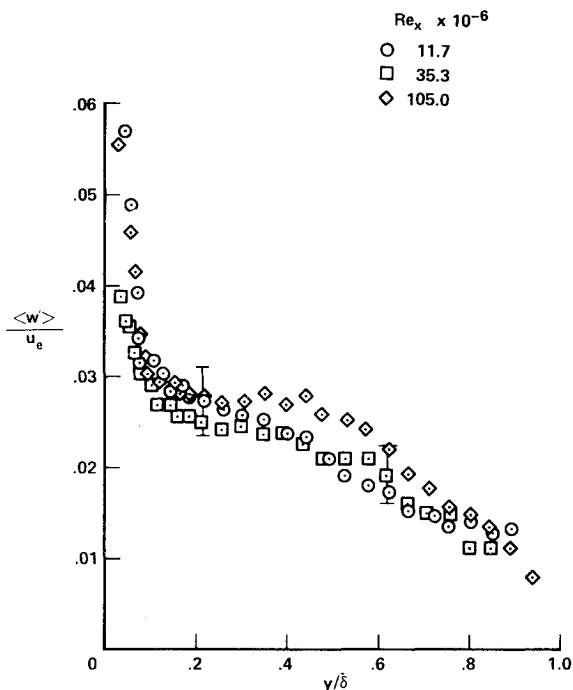


Fig. 8 Distributions of the rms transverse velocity fluctuations for various Reynolds numbers.

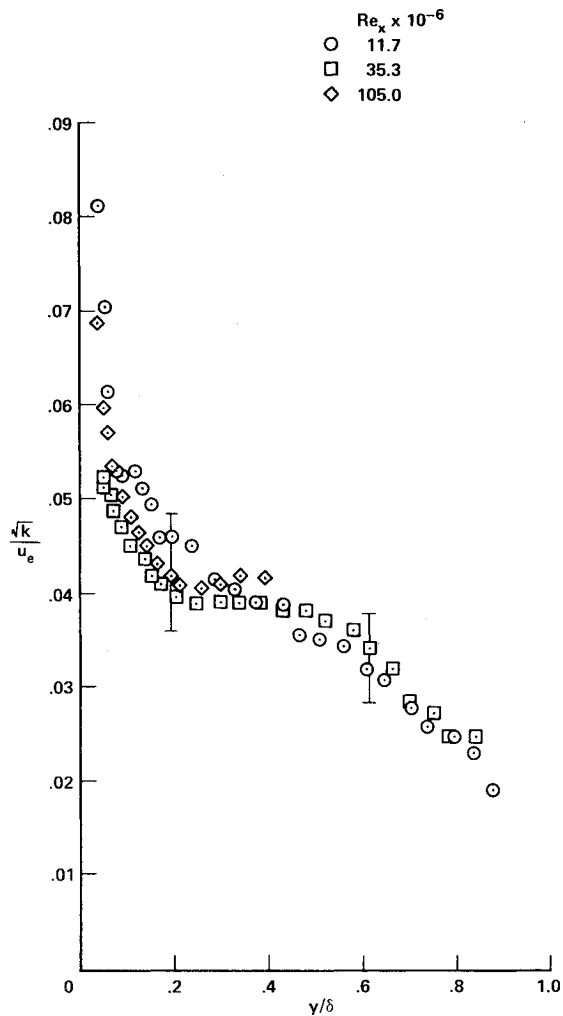


Fig. 9 Distributions of the turbulent kinetic energy for various Reynolds numbers.

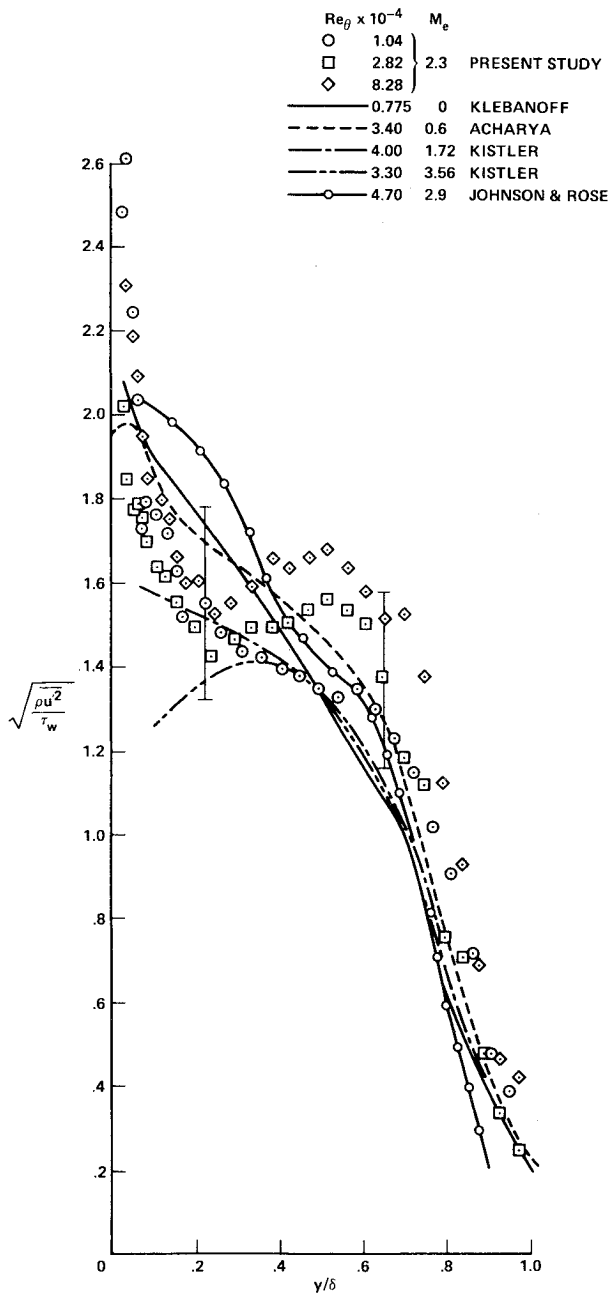


Fig. 10 A comparison of the nondimensional streamwise velocity fluctuations with previous data.

components and turbulent shear stress. The turbulence field measurements reveal one striking feature of supersonic turbulent boundary layers: the magnitude of the transverse and vertical fluctuations are essentially equal throughout the boundary layer, unlike in incompressible flows, where  $\langle w' \rangle$  is greater than  $\langle v' \rangle$  through most of the layer. Other measurements in hypersonic flows show the same behavior. Data taken over a wide range of Reynolds numbers up to a value of  $105 \times 10^6$  lend support to the conclusion that the boundary layer exhibits similarity in the turbulence field (and mean field) at high Reynolds numbers. Such similarity behavior has been suggested by Zoric,<sup>19</sup> among others. The data for the streamwise velocity fluctuations correlate with previous incompressible and compressible data using Morkovin's "universal" scaling to account for compressibility. Significant deviations between the various profiles of available compressible data preclude a similar conclusion for the vertical velocity fluctuation and shear stress data.

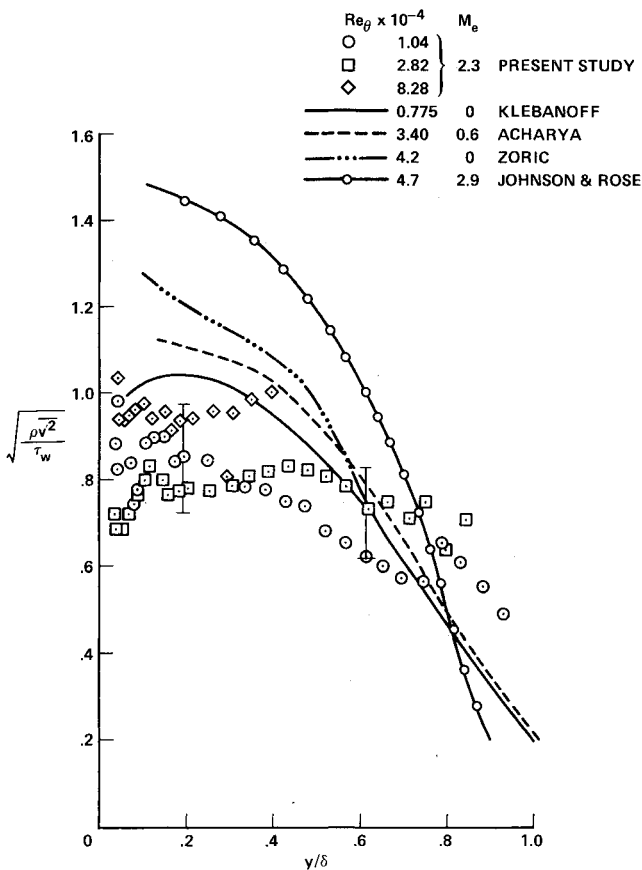


Fig. 11 A comparison of the nondimensional vertical velocity fluctuations with previous data.

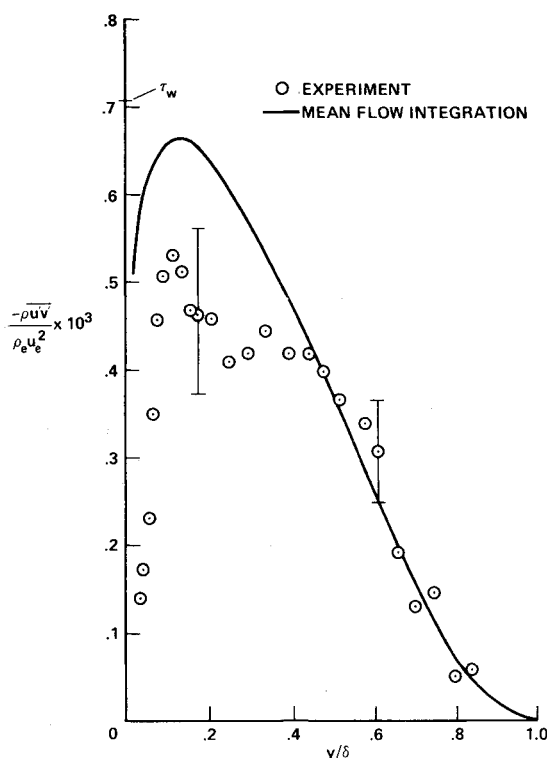


Fig. 12 Turbulent shear stress distribution across the boundary layer,  $Re_x = 35.3 \times 10^6$ .

## References

<sup>1</sup>Sandborn, V.A., "A Review of Turbulence Measurements in Compressible Flow," NASA TM X-62337, March 1974.

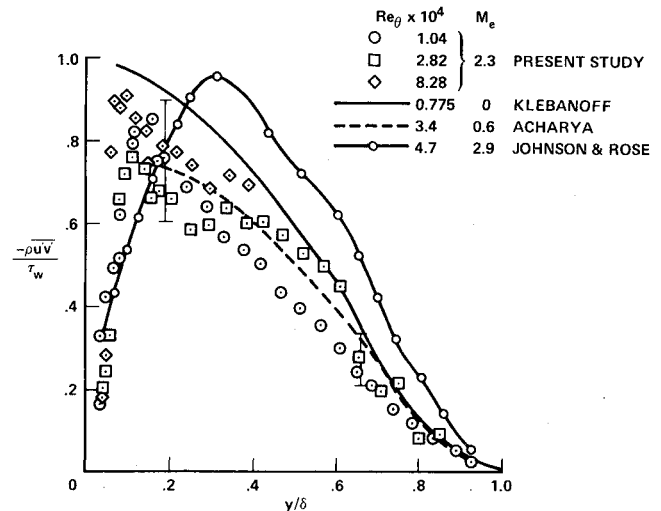


Fig. 13 A comparison of the nondimensional shear stress distributions with previous data.

<sup>2</sup>Marvin, J.G., "Experiments Planned Specifically for Developing Turbulence Models in Computations of Flow Fields Around Aerodynamic Shapes," *AGARD Specialists' Meeting on Numerical Methods and Wind-Tunnel Testing*, Paper 14, Von Karman Institute, Rhode-St-Genese, Belgium, June 23-24, 1976.

<sup>3</sup>Rubesin, M.W., Crisalli, A.J., Horstman, C.C., and Acharya, M., "A Critique of Some Recent Second Order Closure Models for Compressible Boundary Layers," AIAA Paper 77-128, Los Angeles, Calif., Jan. 1977.

<sup>4</sup>Reynolds, W.C., "Computation of Turbulent Flows," *Annual Review of Fluid Mechanics*, Vol. 8, 1976, pp. 183-208.

<sup>5</sup>Acharya, M., Kussoy, M.I., and Horstman, C.C., "Reynolds Number and Pressure Gradient Effects on Compressible Turbulent Boundary Layers," *AIAA Journal*, Vol. 16, Dec. 1978, pp. 1217-1218.

<sup>6</sup>Kussoy, M.I., Horstman, C.C., and Acharya, M., "An Experimental Documentation of Pressure Gradient and Reynolds Number Effects on Compressible Turbulent Boundary Layers," NASA TM 78,488, June 1978.

<sup>7</sup>Morkovin, M.W., "Fluctuations and Hot-Wire Anemometry in Compressible Fluids," *AGARDograph*, No. 24, 1956.

<sup>8</sup>Horstman, C.C. and Rose, W.C., "Hot-Wire Anemometry in Transonic Flow," *AIAA Journal*, Vol. 15, March 1977, pp. 395-401.

<sup>9</sup>Acharya, M., "On the Measurement of Turbulent Fluctuations in High Speed Flows Using Hot-Wires and Hot-Films," NASA TM 78,535, Nov. 1978.

<sup>10</sup>Johnson, D.A. and Rose, W.C., "Laser Velocimeter and Hot-Wire Anemometer Comparison in a Supersonic Boundary Layer," *AIAA Journal*, Vol. 13, April 1975, pp. 512-514.

<sup>11</sup>Coles, D., "Measurements in the Boundary Layer on a Smooth Flat Plate in Supersonic Flow. I. The Problem of the Turbulent Boundary Layer," Jet Propulsion Lab., Calif. Inst. of Technology, Pasadena, Calif., Rept. 20-69, 1953.

<sup>12</sup>Kovaszny, L.S.G., "The Hot-Wire Anemometer in Supersonic Flow," *Journal of Aeronautical Sciences*, Vol. 17, Sept. 1950, pp. 565-572.

<sup>13</sup>Kistler, A.L., "Fluctuation Measurements in a Supersonic Turbulent Boundary Layer," *Physics of Fluids*, Vol. 2, May-June 1959, pp. 290-296.

<sup>14</sup>Klebanoff, P.S., "Characteristics of Turbulence in a Boundary Layer with Zero Pressure Gradient," NACA Rept. 1247, 1955.

<sup>15</sup>Acharya, M., "Effects of Compressibility on Boundary Layer Turbulence," *AIAA Journal*, Vol. 15, March 1977, pp. 303-304.

<sup>16</sup>Mikulla, V. and Horstman, C.C., "Turbulence Stress Measurements in a Nonadiabatic Hypersonic Boundary Layer," *AIAA Journal*, Vol. 13, Dec. 1975, pp. 1607-1613.

<sup>17</sup>Morkovin, M.V., "Effects of Compressibility on Turbulent Flow," *The Mechanics of Turbulence*, Gordon and Breach, New York, 1964, pp. 367-380.

<sup>18</sup>Sandborn, V.A., "Effect of Velocity Gradients on Measurements of Turbulent Shear Stress," *AIAA Journal*, Vol. 14, March 1976, pp. 400-402.

<sup>19</sup>Zoric, D.L., "Approach of Turbulent Boundary Layer to Similarity," Colorado State University, Fort Collins, Colo., Rept. CER 68-69 DLZ 9, 1968.